Theoretical and Experimental Discourse on Laser Ignition in Liquid Rocket Engines

By Chiara Manfletti, Michael Oschwald and Joachim Sender

Institute of Space Propulsion, German Aerospace Center (DLR), Lampoldshausen, Germany

Igniter technologies have seen an increased interest in the past decades due to the increasing re-ignition needs, such as for the upper stage Vinci engine. Weight reduction considerations and redundancy considerations have lead to an increased number of studies in alternative igniter technologies to the conventional pyrotechnical or spark plug igniters in use today. Such technologies include concepts such as resonance igniters, catalyst igniters and laser igniters. When compared to classical ignition methods, both in the automotive industry, i.e. spark ignition, and in the space industry, i.e. pyrotechnic/torch ignition, laser ignition system (LIS) offer multiple advantages.

Literature classifies laser-gas interactions into four main categories which differ in the mechanisms leading to ignition: non-resonant breakdown ignition, resonant breakdown ignition, thermal ignition and photochemical ignition. Non-resonant laser ignition is the most common form of ignition and involves a well-focused pulsed laser beam thus creating a well localized plasma which can accumulate further energy leading to a local increase in temperature and finally ignition. Non-resonant laser ignition may occur via either a multiphoton ionization process or an electron cascade process.

This paper addresses the main issues related with the various laser ignition methods via a literature review of research conducted in the field of laser ignition. The main findings of the experimental work done in the non-resonant laser ignition of a coaxial liquid oxygen and gaseous methane jet at the DLR Lampoldshausen M3.1 test bench is presented.

Nomenclature

a	:	sonic velocity
c	:	speed of sound
d	:	diameter
E	:	energy
g	:	gravitational acceleration
h	:	Planck's constant, $h = 6.626 \cdot 10^{-34}$ J/s
J	:	momentum flux ratio, $J = (\rho v^2)_{fu}/(\rho v^2)_{ox}$
LOx	:	liquid oxygen
$\dot{m}$	:	mass flow
p	:	pressure
M	:	Mach number $M = \frac{v}{a}$
M_R	:	mixture ratio (ratio oxidiser to fuel)
$\mathrm{R_e}$	:	Reylonds number
$\Re$	:	universal gas constant
S_L	:	laminar flame speed
T	:	Temperature
v	:	velocity
v_R	:	velocity ratio (ratio gas to liquid velocity)
We	:	Weber number, $We = \rho_l d(v_g - v_l)^2)/\sigma_l$
α	:	heat diffusivity
λ	:	wavelength
ϕ	:	equivalence ratio, $\phi = M_R/M_{R st}$
ρ	:	density
σ	:	surface tension
τ	:	characteristic time

Subscripts

c	:	chamber
cr	:	critical
fu	:	fuel
i	:	ignition
l	:	liquid
nzl	:	nozzle
$snzl$	:	sonic nozzle
ox	:	oxidiser
$prop$	:	propellant
r	:	residence
st	:	stoichiometric

1. Introduction

Igniter technologies have seen an increased interest in the past decades due to the increasing re-ignition needs, such as for the upper stage *Vinci* engine. Weight reduction considerations and redundancy considerations have lead to an increased number of studies in alternative igniter technologies to the conventional pyrotechnical or spark plug igniters in use today. Such technologies include concepts such as resonance igniters, catalyst igniters and laser igniters. Due to their potential advantages over other technologies, both a resonance igniter and a laser igniter concept would be advantageous for future space propulsion activities.

Whereas investigations into resonance ignition have been limited to laboratory level, significant research has been performed in the area of laser ignition in the past decade at DLR Lampoldshausen.[1,2] With this background knowledge the next step in the technology development process can be made: namely the application to small to medium sized thrusters, i.e. Reaction Control System (RCS) and Orbital Manoeuvring System (OMS) thrusters.

Current RCS and OMS technology is a well established and mature technology based on either a monopropellant and a catalyst or a hypergolic bipropellant combination to provide thrust. These are however far from being considered clean propellants, and the idea of implementing so called "green" propellants has taken on increased weight. Clearly the options available are many and the best solution needs to be determined in order to provide a viable option to current RCS and OMS technology which in turn would lead to a cleaner and at least just as reliable alternative. The best performing non-toxic alternatives to H2 belong to the family of hydrocarbons, i.e. methane, propane and kerosene, and present several advantages like higher density or easier storability at ambient conditions (lower cooling efforts). Known disadvantages, and which are minimised when implementing methane, are their known tendency to produce soot reducing the ISP and a carbon layer at the cooling channel wall, which lowers the cooling efficiency.

Beyond structural weight considerations linked to propellant storage systems required for these alternative "green" propellants, and performance considerations, limited not only to the specific impulse capability of each propellant combination, but more-so to specific impulse to volume ratios, another important issue is ignition. Because these "green" propellants are not hypergolic, an external ignition source must be provided, and this must be reliable, provide for redundancy, whilst maintaining simplicity and be weight-efficient. Without such a reliable ignition system, current RCS and OMS technology will not experience an innovative evolution. When compared to classical ignition methods, both in the automotive industry, i.e. spark ignition, and in the space industry, i.e. pyrotechnic/torch ignition, laser ignition system (LIS) offer multiple advantages.

The current paper, which focuses on rocket propulsion applications, is divided into two main sections. The first gives a general overview of laser ignition and the four different laser ignition methods: thermal, photochemical, resonant, and non-resonant. A brief discussion of ignition overpressure and flame kernel growth follows. The second part of the paper describes the DLR M3.1 microcombustor and the CH_4 Laser campaign conducted to investigate into the laser ignition of coaxially injection liquid oxygen and gaseous methane. Three different families of ignitions are examined: hard, smooth, and transition both in terms of characteristic ignition and injection parameters as well as flame kernel growth during the initial ignition phase.

2. Laser Ignition

Ignition via a laser beam is an external ignition method which offers a number of advantages when compared to other ignition methods. A non-exhaustive list includes: high temporal and spatial precision and accuracy, minimal ignition delay, no need for premixing, simultaneous ignition of multiple combustion chambers via optical fibre coupling, an increased ignition probability for a wider range of mixture ratios and initial chamber conditions (from vacuum to high pressure), as well as an electromagnetic interference (EMI) which is well below permissible levels for space flight.

Studies comparing laser and electric spark ignition for fuel rich mixtures has shown that laser ignition ensures a higher ignition probability for lower pressures and this is independent of the initial chamber pressure.[3]

Laser ignition can be performed in a number of different ways, by direct means, whereby the laser energy is absorbed by the propellants directly upon impingement of the laser beam, or indirectly, whereby the laser energy is transmitted from the laser beam to the propellants via another medium, such as metal particles.

There are four laser ignition methods which can be theoretically implemented: thermal, photochemical, resonant and non-resonant laser ignition. Each method differs in the energy levels required and therefore wavelength region in which they operate. All but the thermal laser ignition are direct ignition methods.

2.1. Thermal Ignition

Thermal laser ignition implements a low energy laser beam, in the infra-red range, which is directed towards a metal target and which thus absorbs the incoming laser energy. Metal particles are set free which then interact with injected propellants confiring them with the energy absorbed. When sufficient energy is thus transmitted, ignition can take place.

Thermal laser ignition has been performed in Japan with the aim of not only measuring the minimum laser energies required to ignite mixtures of gaseous oxygen and methane and gaseous oxygen and hydrogen, but also testing various metals for ablation resistance for RCS applications. The study performed by HASEGAWA presented a number of interesting results. Via a small window in the small rocket chamber wall, a Nd:YAG 1064 nm laser beam was focused on an inner chamber wall. Minimum ignition energies measured were in the range of 1-2 mJ and tantalum demonstrated the best qualities for

thermal laser ignition, losing the least material and for RCS applications which require a large number of cycles, thus best suited.[4]

The advantage of thermal ignition is that it requires only very small ignition energies in the infra-red spectrum range. Thermal ignition can therefore be implemented via either a CO_2 laser or better a Nd:YAG laser. Due to the intensive use made of the latter in many scientific fields, Nd:YAG lasers have seen a tremendous miniaturisation in the last decade. This miniaturisation allows their integration into hardware for weight-sensitive applications such as space propulsion. Figure 1 depicts such a miniaturised Nd:YAG Laser.[5]

Fig. 1: HiPoLas: miniaturised Nd:YAG Laser

2.2. Photochemical Ignition

Photochemical implements a high energy beam such that one photon alone carries enough energy to ionise an atom or molecule. Ionisation potentials of oxygen, hydrogen and methane are given in Table 1. A photon carrying enough energy must therefore be of a specific wavelength or shorter. Using Equation 1 the maximum allowable wavelengths given in Table 1 can be obtained. Photons capable of initiating a photochemical laser ignition are therefore of the Vacuum-UV range or of higher frequencies. No laser system to date exists which is capable of emitting photons in such wavelength ranges.

Table 1: Ionisation Potentials and Maximum Photon Wavelengths

Molecule	Ionisation Pot.	λ_{max}
O_2	12.07 eV	102.73 nm
H_2	15.425 eV	99.12 nm
CH_4	12.51 eV	80.39 nm

$$\lambda <= \frac{hc}{E} \qquad (1)$$

2.3. Resonant Laser Ignition

Via the absorption of a number of lower energy photons, molecules or atoms can be ionised. The ionisation energy required can be minimised if the wavelength of the incoming laser beam is tuned to the two-photon absorption wavelength of the atom which is to be ionised. The resonant multi-photon ionisation process thus becomes the dominant ionisation process. Table 2 lists the two-photon absorption wavelengths of oxygen and hydrogen. These wavelengths are in the UV-C range. Excimer lasers are therefore required.

Table 2: Two-Photon Absorption Wavelengths

Atom	2-Photon Ab. λ
O	ca. 225.6 nm
H	ca. 243 nm

A study by FORCH[6] has shown that indeed the incoming laser energy required can be reduced if the laser beam wavelength is tuned to the two-photon absorption wavelength of one of the atoms of the fluid mixture. His studies concentrate on the oxygen atom. He has shown that the incident laser energy required for ignition shows a strong dependency on the wavelength with prominent features at wavelengths which show flourescence peaks.[6] In[7] FORCH presents his findings for a CH_4/N_2O mixture, where the laser was tuned to the oxygen-atom two-absorption wavelength, 225.6 nm: successful ignition was obtained for energies as low as 0.65 mJ.

Further investigations highlighted the importance of the laser-oxidiser interaction in the ignition process of an H_2/O_2 mixture. In a comparison between the incident laser energy required for ignition of an H_2/O_2 mixture with a 225.6 nm beam and a 532 nm beam (Nd:YAG 2nd harmonic) for different mixture ratios, it was demonstrated that the former required as little as ca. 0.3 mJ whilst the latter required ca. 13 mJ.[6] It is significant to note that this minimum is located in fuel rich regions far from stoichiometry in contrast to what is normally observed in spark ignition. In their paper the authors discuss the photochemical formation of radicals in the converging laser beam near the plasma created as possibly playing a major role in the early stages of flame growth once the plasma has decayed.

2.4. Non-Resonant Laser Ignition

Non-resonant ignition, is together with the thermal ignition, one of the more viable laser ignition methods. A high energy beam is focused in a small volume creating a local electric field which, interacting with the gas molecules, causes breakdown of the molecules. Ionisation occurs via the multiphoton ionisation process and the ensuing electron avalanche. The local electric field strength increases as the avalanche magnitude increases and continues to do so until the ionisationsation potential of the medium is exceeded; plasma breakdown occurs and local temperatures as high as 10^6 K. One of the advantages of non-resonant laser ignition for space applications is that Nd:YAG laser may be implemented, which thanks to their miniaturisation level are not associated with a undesirable weight penalty. On the other hand, energies required for this type of laser ignition are significantly higher than

those necessary for aforementioned thermal, resonant, photochemical ignition types. It is this type of ignition which has been implemented at DLR Lampoldshausen in past investigations into laser ignition of various propellant combinations.

3. Ignition Characteristics

A great number of studies examine the growth of the initial flame kernel of pre-mixed flames after ignition via laser. Clearly the growth of this initial kernel is influenced by the flame nature itself. In rocket engines, premixed diffusion flames are not relevant as the mixing of the propellants occurs after injection of these into the combustion chamber. Combustion is therefore not only dictated by activation energies of the propellants and their characteristic reaction times, but also by characteristic mixing times, propellant velocities, velocity ratios and impulse flux ratios (J). In liquid rocket engines additional factors increase the complexity of the problem at hand as the propellants, being injected in their liquid or supercritical states, must first evaporate or gasify before combustion may take place. The conditions under which a flame kernel grows in rocket propulsion applications are therefore significantly harsher as the flames are turbulent non pre-mixed flames.

The preferred method of ignition in liquid rocket engines of higher thrust-classes in Europe has been that of pyrotechnic ignition. A pyrotechnical charge is ignited and the resulting hot gases are directed to the main combustion chamber where they are injected centrally. A pilot flame is thus created which reacts with the freshly injected liquid propellants and ignites the main combustion chamber as the flame expands radially.

The pilot flame provides the necessary ignition energy, and when compared to a single laser pulse of a duration of 10 ns which is focused into the combustion chamber, it represents an energy source which is present over an extended period of time and over an extended surface area. This energy source can therefore be said to be located at different locations along the axial path along which the injected propellant jets interact, break-up, mix and finally react.

3.1. Flame Kernel Growth

For a flame kernel to develop into a stationary flame, its size must reach a so-called critical diameter, d_{cr}, beyond which, it will grown unaided, i.e. without additional external energy. Clearly, initial flame kernels which develop under the aid of a pilot flame are fed with additional energy even after they have attained their critical diameter. The manner and location of energy addition is thus not as critical as some initial flame kernels are extinguished while others grow aided. In the case of laser ignition the energy is transmitted very locally both in space as well as in time.

As only one flame kernel ensues at the location where the laser beam is focused, it is therefore of the utmost importance that this transmission be done at the most promising location to ensure that the flame kernel attains its critical diameter and that the laminar flame speeds which results are enough to compensate for the heat losses which occur via conduction.

One of the most important parameters when considering the direct ignition of the combustion chamber is the location where the laser beam is focused. Figure 2 depicts two injected coaxial streams and the resulting mixing layer which forms with possible laser focusing locations which, depending on injection conditions, might lead to successfull ignition.
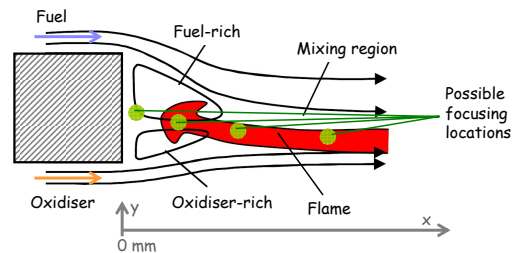

Fig. 2: Mixing Region in the Shear Layer of Two Coaxial Jets and Laser Focusing Locations

Equation 2 describes the flame growth rate for a standard case as a function of the laminar flame speed and the dissipation heat losses, where C is a constant and is equal to 12 for a spherical pocket.[8]

$$\frac{d_{cr}S_L}{\alpha} = C \qquad (2)$$

In a turbulent mixing flame, the location of the flame kernel, and its growth is also a function of the velocity of the injected propellants and more so of the jet of highest impulse.

In Section 5 the flame front velocities and flame growth will be discussed in further detail.

3.2. Ignition Over-Pressure

One of the most important parameters used to characterise ignition and the various ignition methods, is the ignition delay, i.e. the time required before a successful ignition takes place. A failed ignition leads to accumulation of un-burnt propellants in the combustion chamber volume. This is undesirable as these will mix and a subsequent ignition may turn out to be deflagration or detonation-like. Such ignition types are characterised by high ignition pressure peaks which are significantly higher than the desired nominal combustion chamber pressure. This peak pressure is also known as ignition overpressure and may be estimated using Equation 3.[8]

$$p_{max} = p_c \frac{\overline{\dot{m}_i \tau_i}}{\overline{\dot{m}\tau_r}} \qquad (3)$$

The peak overpressure is therefore a function of the accumulated masses, i.e. the time between the opening of the propellant valves and the laser beam pulse focusing inside the combustion chamber. In such cases, the entire accumulated propellant mass is combusted instantaneously. Should the chamber pressure increase above the dome pressures, as is occurs in the case of extreme overpressures, a blockage of the injected propellants occurs, no new fresh propellants are fed and the flame is extinguished. Such an ignition is known as a "hard ignition". In less extreme cases, blockage of the injector is short-lived and fresh propellants are injected before the flame is completely extinguished. This allows, the flame, which has moved downstream towards the nozzle, to again expand and move towards the injector faceplate where it will anchor if the right injection conditions exist (ratio between J and We).[1] Ideally, as is the case during "smooth ignition" the initial flame kernel develops gradually into the steady-state flame with no ignition overpressure. In the CH_4 Laser Campaign both ignition types were encountered.

4. Experimental setup

4.1. M3.1 Hardware

The CH4-Laser campaign made use of the M3 Micro-combustor whose two most important features are the wide optical quartz windows which provide a complete optical access to the combustion chamber and the small windows located in the upper part of the chamber are used to allow the access of the converged laser beam to the chamber. The micro-combustor is a horizontally mounted combustion chamber (CC). The section of the combustion chamber is rectangular with dimensions: 60 x 60 x 140 mm.
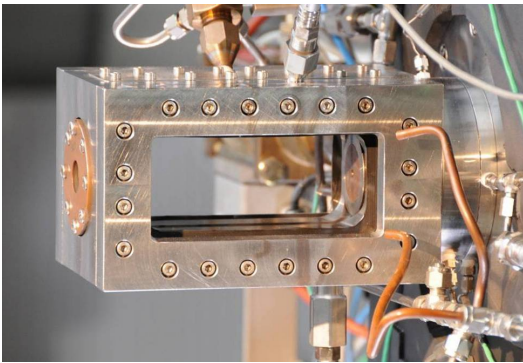

Fig. 3: M3.1 Microcombustor

The combustion chamber design allows the installation of a multitude of different injector elements. In this case use was made of a single coaxial injector with no recess or tapering. Varying of the co-axial element diameters

is possible, allowing flexibility in terms of injection conditions which can be achieved. Additional geometric variations can be made in both the exit nozzle, in order to fix the total mass flow rate, and in the sonic nozzle used to determine the mass flow rate of the gaseous propellants. Thanks to a liquid nitrogen bath injection of liquid oxygen is possible. Maximum feed pressures are 40 bar and maximum liquid mass flows are ca. 400 g/s.

4.2. Single Injector Head

The M3.1 injector head configuration is depicted schematically in Figure 4. Table 3 summarises the general dimensions of the two injector configurations implemented for this campaign.

Table 3: Injector Head Geometric Details

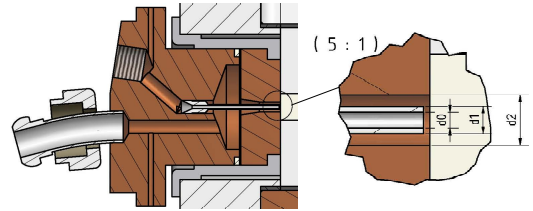| Geometry	Conf. 1	Conf. 2
LOx post inner diam., d_0	1.6 mm	1.6 mm
LOx post outer diam., d_1	2.4 mm	2.4 mm
Fuel orfice diam., d_2	5.0 mm	6.0 mm
Fuel sonic nozzle throat diam., d_{snzl}	2.05 mm	2.05 mm
Main nozzle throat diam., d_{nzl}	17 mm	25 mm

Fig. 4: M3.1 Micro-combustor Injector Head Schematics

4.3. Ingnition Sequence

Figure 5 depicts, schematically, the sequence used in the CH_4-Laser Campaign. Prior to testing, the combustion chamber is purged with nitrogen. The fuel valve is opened first and the combustion chamber is partially conditioned with gaseous methane. Subsequently the main liquid oxygen valve is opened and a steady state jet is established in the chamber. At $t = 0$ s the laser beam is focused into the chamber and ignition occurs shortly afterwards.
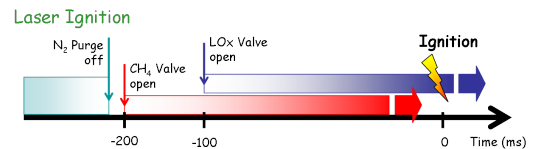

Fig. 5: M3.1 Micro-combustor Injector Head Schematics

4.4. Laser Nd:YAG

The laser implemented for ignition, is a table top Nd:YAG laser. Beam laser energies are in the range 70-110 mJ,

with laser pulse durations of 10 ns. The laser source is located at some distance from the micro-combustor and is focussed into the chamber thanks to a number of mirrors and lenses. The final lens has a focal length of 60 mm. In this campaign the laser was focused at ca. 27 mm from the injector face place and at 2 mm from the chamber central axis, i.e. in the shear layer between the two coaxially injected jets.

4.5. Optical Diagnostics

The CH_4-Laser campaign made use of high speed imaging: spontaneous OH emission and shadowgraph. A classical Z-setup was implemented as depicted in Figure 6. Details of the camera settings implemented are summarised in Table 4.
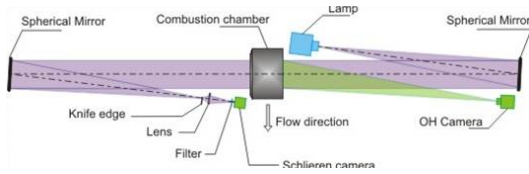
Fig. 6: Optical Z-Setup

Table 4: Camera Settings

Settings	OH	Shadowgraph
Lens	UV-Nikkor 105 mm	none
Filter	OH Filter	SZS20, T = 0.1
Gain (V)	3.4 - 3.6	none
Frame rate (fps)	12500	9000
Resolution (pixel)	512 x 256	512 x 192
Shutter	1/frame	1/657000

5. Experimental Results

5.1. CH_4-Laser Campaign

Table 5 summarises the main parameters which describe the campaign conducted. Hot flow conditions are averaged over a period of 200 ms towards the end of the test run when steady-state conditions are reached. Cold flow conditions are the near instantaneous conditions just prior to incoming of the laser beam. The latter are of course fundamental for this study as it is in these conditions that the initial flame kernel or initial plasma created by the laser beam is to develop.

5.2. Smooth and Strong CH_4 Laser Ignition

In the CH_4-Laser Campaign, both smooth and hard ignitions have been observed. An additional transition type has been observed which falls between the two extreme cases. Figures 7 - 9 depict OH images for each type of ignition, whereas Figure 10 depicts shadowgraph images

Table 5: Average O_2/CH_4 Laser Campaign Parameters

	Hot	**Cold**	
Prop. comb.		LOx/GCH$_4$	
M_R	3.4 - 4.7	3.3 - 7.9	
ϕ	0.87 - 1.18	0.85 - 1.98	
$\dot{m}_{tot}$	26.8 - 71.9	27.8 - 93.4	g/s
p_c	1.7 - 2	0.91 - 0.99	bar
p_{ox}	3.1 - 12.4	2.3 - 6.3	bar
T_{ox}	87 - 98	86 - 110	K
p_{fu}	2.3 - 4.1	2.0 - 4.0	bar
T_{fu}	222 - 253	184 - 252	K
v_{ox}	9 - 24	9 - 33	m/s
v_{fu}	226 - 375	330 - 386	m/s
J	0.26 - 1.27	0.25 - 1.74	
We	10 180 - 24965	15700 - 43000	

of the initial flame kernel displacement for a hard ignition case. Table 6 summarises the values for these ignition plots and Figure 11 summarises the J and We values for all ignition types encountered in the CH_4-Laser Campaign.
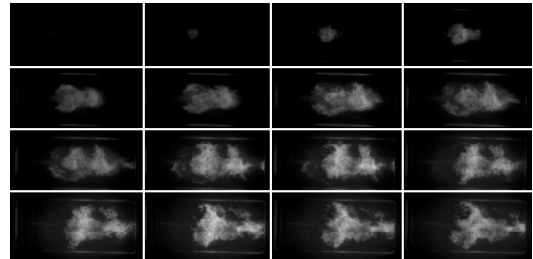

Fig. 7: Smooth Ignition Type: OH Image Series, dt = $1.1 \cdot 10^{-1}$ ms

The series of images depict the plasma created by the incoming laser beam, the subsequent downstream displacement of the initial flame kernel and its growth. It becomes clear that, the rate of flame growth changes during the ignition transient and does not obey a linear law. By simple observation of the images two facts become clear: a) the focus of the flame kernel is displaced about 1/5 of the chamber length in 0.33 ms and b) the growth of the kernel is not symmetric in the upstream and downstream directions. It becomes clear that additional parameters need to be taken into consideration to describe the ignition process. Clearly the flame growth process is initially slower than the averaged flow dynamics.

Figure 11 displays the J and We numbers for all tests performed (unfilled symbols are We numbers). It becomes clear hard ignitions are characterised by high We (ca. $35 \cdot 10^3$ - $45 \cdot 10^3$) and low J numbers whereas smooth ignitions display higher J numbers and lower WEBER numbers (ca. 3 times lower). The family of transition ignitions, which display characteristics of both smooth and hard ignitions, is characterised by low J and low We numbers.
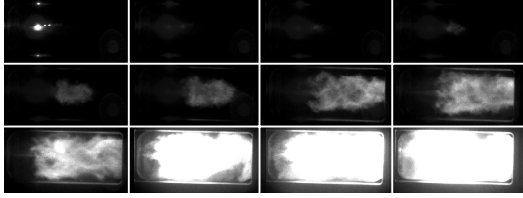
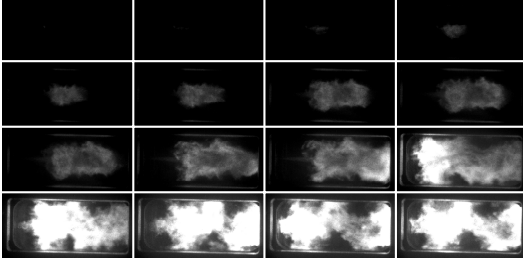Fig. 8: Hard Ignition Type: OH Image Series, dt = $1.1 \cdot 10^{-1}$ ms

Fig. 9: Transition Ignition Type: OH Image Series, dt = $1.1 \cdot 10^{-1}$ ms
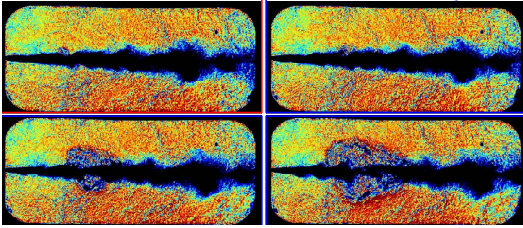

Fig. 10: Laser Pulse in a Coaxial LOx/CH$_4$ Jet and Flame Kernel Growth with dt = $1.1 \cdot 10^{-1}$ ms

Table 6: Smooth and Hard Ignition Parameters (LOx/GCH$_4$) at t = 0 s

	Smooth	**Hard**	**Transition**	
Test run	27-14	29-05	27-07	
Injector conf.	1	2	1	
M_R	4.5	3.55	5.25	
ϕ	1.13	0.89	1.32	
$\dot{m}_{tot}$	29.1	61.0	40.0	g/s
p_c	0.97	0.94	0.99	bar
$p_{c_{max}}$	3.04	9.388	10.12	bar
p_{ox}	2.8	4.9	2.2	bar
T_{ox}	89.7	107.6	89.4	K
p_{fu}	2.15	3.82	2.2	bar
T_{fu}	191.3	197	187.4	K
v_{ox}	11.6	19.7	14.0	m/s
v_{fu}	336.3	341	332.8	m/s
J	1.0	0.69	0.72	
We	17 342	40644	17392	
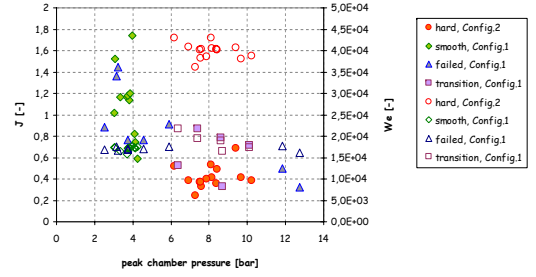
Fig. 11: J and WEBER Numbers vs. Ignition Overpressure

The ignition sequences shows that hard and smooth ignitions different not only in their ignition overpressures, $p_{c_{max}}$, We and J numbers, but also in the flame evolution in the constantly varying pressure and velocity field. To this purpose, and to quantitatively describe differences between each ignition type, the flame fronts for three typical ignitions (hard, smooth, and transition) are shown. Figures 13 - 16 depict the evolution of the upstream and downstream flame fronts and the maximum intensity encountered along the microcombustor centreline.
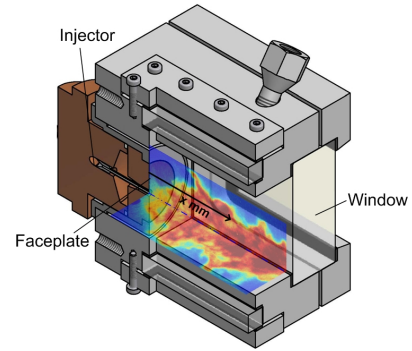

Fig. 12: 3D CAD Schematics of the M3.1 Microcombustor

After the initial laser pulse and associated plasma is detected, no flame is seen. The flame is again detected further downstream for all ignition cases. For smooth ignition cases, the flame moves downstream and then slowly makes its way towards the faceplate.

Hard ignitions are characterised by a sudden expansion of the flame as the propellants are instantaneously combusted. The flame occupies the entire combustion chamber volume, the chamber pressure having increased above dome pressures, causes a blockage and no fresh propellants are injected.

Transition ignitions are also characterised by an initial downstream displacement of the initial flame kernel followed by a fast expansion of the flame. The latter is however less abrupt than in hard ignitions (though ignition overpressures may be of similar magnitude)
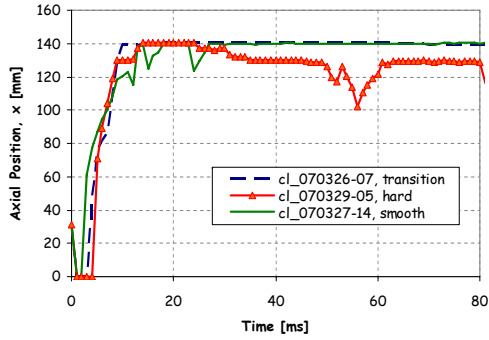
Fig. 13: Upstream Flame Front Evolution for Hard, Smooth, and Transition Ignition Types Along the Microcombustor Centerline
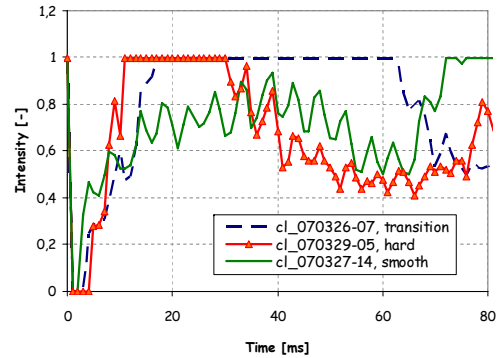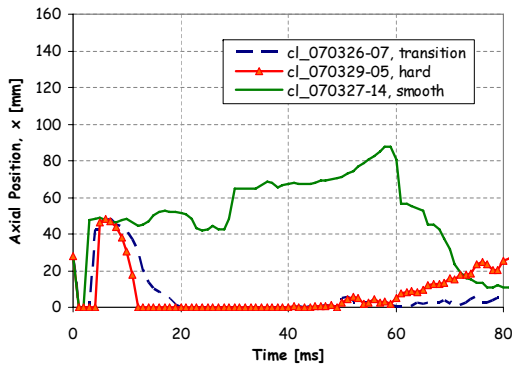

Fig. 14: Downstream Flame Front Evolution for Hard, Smooth, and Transition Ignition Types Along the Microcombustor Centerline
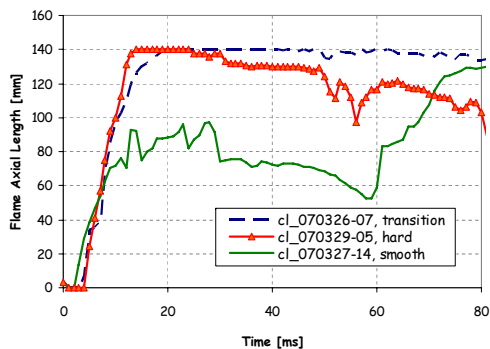

Fig. 15: Downstream Flame Front Evolution for Hard, Smooth, and Transition Ignition Types Along the Microcombustor Centerline

and the flame does not occupy the entire chamber volume. Injector blockage is only short-lived and the flame can then stabilise more rapidly than in hard ignition cases.

Fig. 16: Maximum Flame Intensity Evolution for Hard, Smooth, and Transition Ignition Types Along the Microcombustor Centerline

By implementing the upstream and downstream flame front positions the flame growth rate can be obtained and compared to the value given by

When examining the ignition sequences and the parameters at $t = 0$ s, it becomes clear that harder ignitions are associated with a higher peak pressure. According to studies performed in the past this is related to the ignition delay and the mass of the propellants present in the combustion chamber prior to ignition.[1]
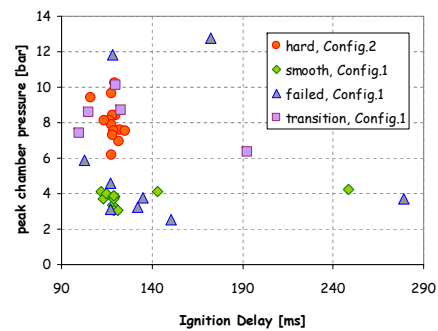

Fig. 17: Relationship between the Ignition Overpressure and the Ignition Delay

Figure 17 depicts the relationship for all tests performed between the peak chamber pressure, or ignition over pressure, and the ignition delay whereas Figure 18 depicts the massflow vs. the ignition overpressure.

Here we can clearly see that hard ignitions are associated with higher mass flows for constant ignition delay, thus confirming past findings. There exists however a family of tests which although characterised by a low ignition delay and a low initial mass flow, display high ignition overpressures. These represent a transition region between smooth and hard ignition and indicate that the
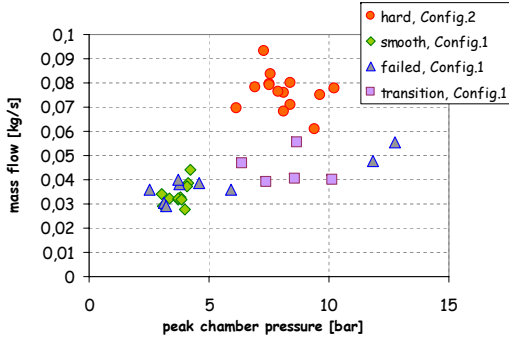
Fig. 18: Relationship between the Mass Flow and the Ignition Overpressure

mass of unburnt propellant present in the chamber alone does not suffice to discern between ignition with high or low ignition overpressures.
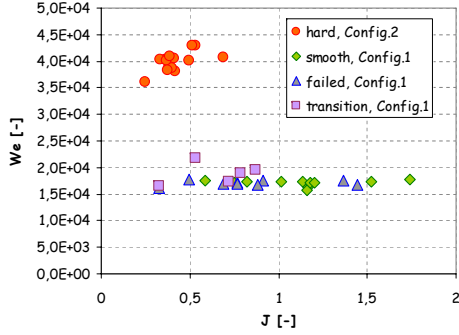

Fig. 19: WEBER over the Momentum Flux Ratio, J

Examining just the relationship between the momentum flux ratio and the WEBER number presented in Figure 19 regions become apparent. In order to determine whether given J and We numbers (as indicated in the figure to be around 1 for impulse flux ratios and between $25 \cdot 10^3$ - $35 \cdot 10^3$ for the WEBER number) constitute boundaries across which ignition types vary from smooth to hard over a transition region additional tests need to be performed.

If the relationship between the oxidiser and fuel MACH numbers is examined it can be seen that the hard ignition correspond to higher oxidiser MACH numbers. As however, prior to ignition, the fuel is injected at sonic speed such that $M_{fu} = 1$ for all tests, such a plot is not of particular interest. Interesting is however the relationship between the oxidiser MACH number and J. In Figure 20 a clear tendency is visible where the transition tests with the highest ignition overpressures are those closest to the hard ignition region in the upper left region of the graph.

Interestingly enough depiction of the OHNESORGE number, which represents the relationship between the friction and surface tension forces, against the liquid
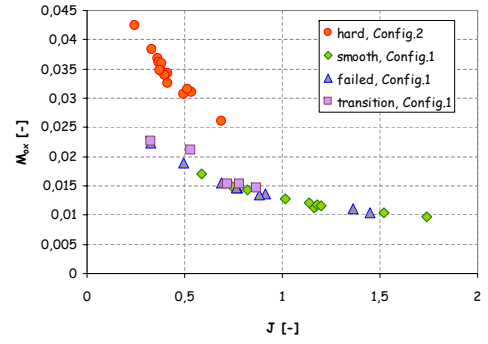

Fig. 20: Relationship between the LOx MACH Number and the Momentum Flux Ratio
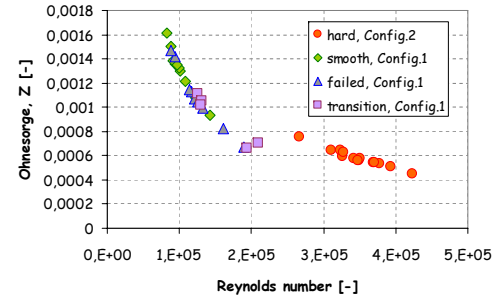

Fig. 21: Relationship between the OHNESORGE Number and the LOx REYNOLDS Number

oxygen REYNOLDS number (Figure 21), a plot which is normally used to determine the current jet break-up regime (RAYLEIGH, 1st wind, 2nd wind, or atomisation), displays very much the same trend.

6. Conclusion and Outlook

Laser ignition is a promising new technology which allows the exact timing of ignition thus reducing the ignition delay. A number of different laser ignition methods exist: thermal, photochemical, resonant, and non-resonant. The most investigated method for space applications is the non-resonant ignition as this allows the use of miniaturised Nd:YAG laser: a significant advantage for weight-saving considerations. Implementation of a non-resonant laser system implies that the coupling of the laser beam to the combution chamber must be performed according to a number of different considerations. The location where the laser beam is focused must be accurately chosen where this would preferably be the mixing layer which is self-established in coaxially injected propellants. Furthermore, the injection conditions at the time of ignition must be selected such as to avoid hard ignitions. Previous studies investigating into the laser ignition of coaxially injected gaseous O_2 and gaseous CH_4 showed that the main difference between hard and smooth ignition was in the mass accumulated in the combustion chamber

References

1) Sender, J., Manfletti, C., Oschwald, M., and Pauly, C., "Ignition Transients of a Gaseous CH4/O2 Coaxial Jet," in *22nd European Conference on Liquid Atomization Spray Systems*, 2008, iLASS08-A109.

2) Razafimandimby, T., De Rosa, M., Schmidt, V., Sender, J., and Oschwald, M., Laser ignition of gh2/lox spray under vacuum conditions, *Proceedings of the European Combustion Meeting* p. 6 (2005).

3) McIntyre, D., *A Laser Spark Plug Ignition System for a Stationary Lean-Burn Natural Gas Reciprocating Engine*, Ph.D. thesis, West Virginia University (2007).

4) Hasegawa, K., Kusaka, K., Kumakawa, A., Sato, M., and Tadano, M., "Laser Ignition Characteristics of GOX/GH2 and GOX/GCH4 Propellants," in *Joint Propulsion Conference*, 2003, aIAA 2003-4906.

5) Grasser, S., Ctr carinthian tech research ag: Agk1 competence centre for advanced sensor technologies, Presentation (June 09, 2009), eSA ESTEC, Noordwijk, The Netherlands.

6) B.E. Forch, A. M., Ultraviolet laser ignition of premixed gases by efficient and resonant multiphoton photochemical formation of microplasmas, *Combustion, Science and Technology* **52**, 151–159 (1987).

7) Forch, B., Resonant laser ignition of reactive gases, *SPIE* **2122**, 1118–128 (1994).

8) Yang, V., Hbiballah, M., Hulka, J., and Popp, M., editors, *Liquid Rocket Thrust Chambers: Aspects of Modeling, Analysis, and Design*, 2004, vol. 200 of *Progress in Astronautics and Aeronautics*, pp. 405–435.

Contact: **chiara.manfletti@dlr.de**